J Mater Sci (2008) 43:1769–1775
DOI 10.1007/s10853-007-2408-x

Preparation of well-dispersed spherical nickel powders with uniform size via mild solvothermal route

Liuyang Bai · Fangli Yuan · Qing Tang ·
Jinlin Li · Hojin Ryu

Received: 20 September 2007 / Accepted: 13 December 2007 / Published online: 18 January 2008

Abstract Well-dispersed spherical nickel powders with uniform size were synthesized via a mild solvothermal route in which aqueous hydrazine was used as reducing agent without any alkaline reagent or surfactant introduced. The as-prepared products were characterized by XRD, FESEM, XPS, and TG. Different influencing factors including solvent, concentration, reaction time, and temperature on the morphology and size of the final products were examined. The size of the spherical nickel powders is tunable from 150 to 800 nm. The obtained nickel powders have little $Ni(OH)_2$ on the surface and exhibit excellent oxidation resistance. In addition, the formation process was discussed on the basis of the experimental results.

Introduction

With the development of base–metal–electrode multilayer ceramic capacitor (BME-MLCC), nickel powders have attracted increasing attention as the substitute for noble metal Pd or Pd/Ag used in the internal electrode of MLCC due to their good electrical conductivity, high melting point, and low cost. Nickel powders as electrode material must be prepared as non-agglomerated spheres with narrow size distribution and high crystallinity [1, 2]. The thickness of the electrode layer in MLCC is about 2 μm, and the ideal diameter of the powders is about 1 μm. However, as the trend in MLCC continues toward miniaturization and high capacitance, nickel powders with smaller size would be desired [3]. A variety of techniques, such as chemical vapor deposition, wet chemical reduction, microwave-assisted hydrothermal method, thermal plasma, polyol process, and spray pyrolysis, have been employed to produce nickel powders. Thermal plasma and spray pyrolysis can produce spherical and well-distributed nickel powders, but expensive equipments are involved [4, 5]. Vapor phase reduction is also an efficient process for production of spherical nickel powders except that some much coarser particles are often included in the products. So further classification is necessary [6]. Chemical solution methods have better capability for controlling composition, size and shape of metal powders and are suitable for scaling up [7–9]. Polyol process is an effective approach for the preparation of well-dispersed metal particles in the micron and submicron size range [10, 11]. But polyol is too expensive as a reductant. Hydrazine (N_2H_4) is a powerful cheap reductant widely used for the production of fine metallic powders. The reducing capability of N_2H_4 is highly dependent on the pH value of the solution. The suitable basic environment was available by adding $NaOH/Na_2CO_3$ into the solution [12, 13]. However, Sodium ion is difficult to remove and can deteriorate the properties of the products. There are also reports on the fabrication of nickel powders without using $NaOH/Na_2CO_3$ as pH value controller. For example, Z. Gui synthesized single crystal nickel nanowhiskers precipitated from $[Ni(NH_3)_4]^{2+}$

L. Bai · F. Yuan (✉) · Q. Tang · J. Li
State Key Laboratory of Multi-phase Complex System, Institute of Process Engineering, Chinese Academy of Sciences,
Beijing 100080, P.R. China
e-mail: flyuan@home.ipe.ac.cn

L. Bai
Graduate University of Chinese Academy of Sciences,
Beijing 100049, P.R. China

H. Ryu
Advance Material Division, Korea Research Institute of Chemical Technology, P.O. Box 107, Yusong-Gu,
Taejeon 305-600, South Korea

solution using N_2H_4 as a reducing agent [14]. C. L. Jiang prepared flower-like microstructures via aqueous solution process employing only $NiCl_2 \cdot 6H_2O$ and $N_2H_4 \cdot H_2O$ as starting materials [15].

In this work, we demonstrated that well-dispersed spherical nickel powders with uniform size could be obtained via a mild solvothermal route without any NaOH/Na_2CO_3 introduced. It was found that the solvent played the key role on the morphology of the products. The size of the spherical nickel powders could be controlled by varying the initial concentration of $NiCl_2 \cdot 6H_2O$ and the reaction temperature.

Experimental

All analytical chemical reagents were obtained from Beijing Chemical Reagents Co. and used without further purification. Typically, an appropriate amount of $NiCl_2 \cdot 6H_2O$ was dissolved into 60 mL of solvent to get homogeneous solution. Then an appropriate amount of $N_2H_4 \cdot H_2O$ (85 wt.%) was added drop-wise into the $NiCl_2 \cdot 6H_2O$ solution. The mixture was sealed in a Teflon-lined autoclave of 100 mL capacity and heated in an oven for 3–8 h. After cooled to room temperature naturally, the precipitates were filtered off and washed with distilled water and anhydrous ethanol in sequence and then dried at 60 °C overnight.

The crystalline phase of the as-prepared samples was characterized by X-ray diffractometry (XRD, X'pert PRO, Panalytical, CuKα radiation) in a 2θ range from 10° to 110°. Their size and morphology were inspected with field scanning electron microscopy (FESEM, JEOL JSM-6700F). Surface of nickel powders was analyzed by X-ray photoelectron spectroscopy (XPS, VG Scientific ESCA-Lab220i-XL) using 300 W AlKα radiation. The thermal stability of the products was recorded using a thermal analyzer (Netzsch STA 449 TG-DTA/DSC) in air with the heating rate of 10 °C/min up to 900 °C.

Results and discussion

Formation of nickel powders

The conventional reduction process of nickel using hydrazine as a reducing agent in the presence of NaOH/Na_2CO_3 was given in the literature as Eq. 1 [16] and Eq. 2 [17]

$$2\left[Ni(N_2H_4)_3\right]^{2+} + 4OH^- \rightarrow 2Ni(s) + N_2(g) + 4H_2O + 5N_2H_4 \quad (1)$$

$$2Ni(OH)_2 + N_2H_4 \rightarrow 2Ni + N_2(g) + 4H_2O \quad (2)$$

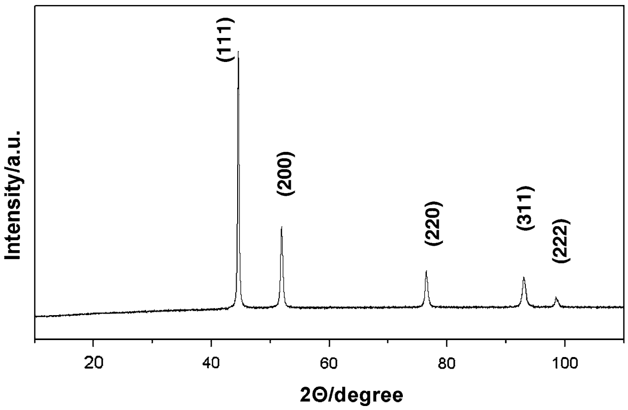

Fig. 1 XRD patterns of the prepared metallic nickel powders

However, without NaOH/Na_2CO_3 being introduced, the formation of metallic nickel powders could also be achieved by hydrazine reduction via solvothermal route. Figure 1 shows the typical XRD pattern of the solid product obtained in glycerin solution at 120 °C for 6 h with the concentration of nickel and hydrazine at 0.1 and 0.6 M, respectively. The five diffraction peaks of (111), (200), (220), (311), and (222) of face-centered cubic (fcc) Ni can be easily observed. No peaks of nickel oxide or hydroxide are detected, indicating that pure fcc Ni was obtained under such experimental condition. The sharp diffraction peaks indicate the as-synthesized nickel powders of good crystallinity.

When the experiment was performed using similar procedure except that no hydrazine was added and ammonia/NaOH was introduced as pH controller, no nickel powders were formed. It reveals that it was hydrazine instead of glycerin that reduced nickel from solution, which was further confirmed by the FT-IR absorption spectra of the post-reaction liquid. Plots (a) and (b) in Fig. 2 are the FT-IR absorption spectra of the filtrate of the post-reaction solution and pure glycerin, respectively. In order to

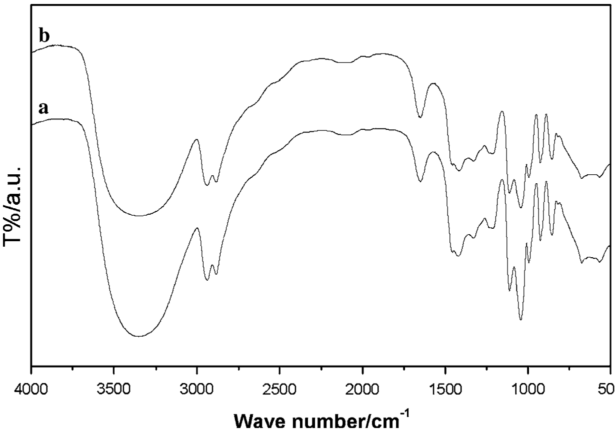

Fig. 2 FT-IR absorption spectra of the filtrate of post-reaction solution (**a**) and pure glycerin (**b**)

concentrate the possible products in the solution, the experiment was performed with much higher reactant concentration ([Ni^{2+}] = 0.5 M) and longer reaction time (12 h). It can be seen that these two spectra are greatly similar, and no absorption at 1,700–1,750cm^{-1} attributed to the typical absorption of C=O stretch vibration exists in plot (a), indicating glycerin was not involved in the reduction reaction. Therefore, glycerin can be recycled as the reaction media. The reaction process can be simply formulated as a complexation–reduction process given below [18]:

$$\mathrm{Ni^{2+} + 3N_2H_4 \rightarrow \left[Ni(N_2H_4)_3\right]^{2+}} \quad (3)$$

$$\mathrm{\left[Ni(N_2H_4)_3\right]^{2+} + N_2H_4 \rightarrow Ni(s) + 4NH_3(g) + 2N_2(g) + H_2 + 2H^+} \quad (4)$$

Effect of solvent

The solvent had great effect on the morphology of the products. Figure 3 shows the FESEM images of products obtained at 120 °C for 6 h fixing the concentration of nickel and hydrazine at 0.1 and 0.6 M when water, ethanol, ethylene glycol, and glycerin were used as solvents, respectively. Figure 3a and b are the images of the product precipitated from glycerin solution. The spherical nickel particles are well dispersed and have uniform diameter of about 300 nm. Compared with that shown in Fig. 3a and b, the product precipitated from ethylene glycol is also composed of well-dispersed particles with uniform size, but the shape of them exhibits only quasi-spherical as shown in Fig. 3c. Figure 3d shows the FESEM image of that precipitated from aqueous solution. The particles exhibit flower-like shape with some nanotips extending from the cores. It is reported that the dielectric constant of solution influences the morphology of resulting powders [19]. So the variation of the morphology could be attributed to the difference of the dielectric constant of the solution. Monodisperse spherical nickel powders with uniform size could be obtained in glycerin as reaction media with no surfactant introduced.

Effect of concentration

In order to find out the effect of concentration on the morphology and size of resulting nickel powders, the reduction was performed at 120 °C for 6 h with various concentrations of nickel ion and hydrazine. Figure 4a and b shows the FESEM images of products obtained with the concentrations of nickel at 0.075 and 0.05 M while fixing the concentration of hydrazine at 0.6 M. The products are both composed of spheres. The average diameter of the products is 500 nm at 0.075 M and 800 nm at 0.05 M.

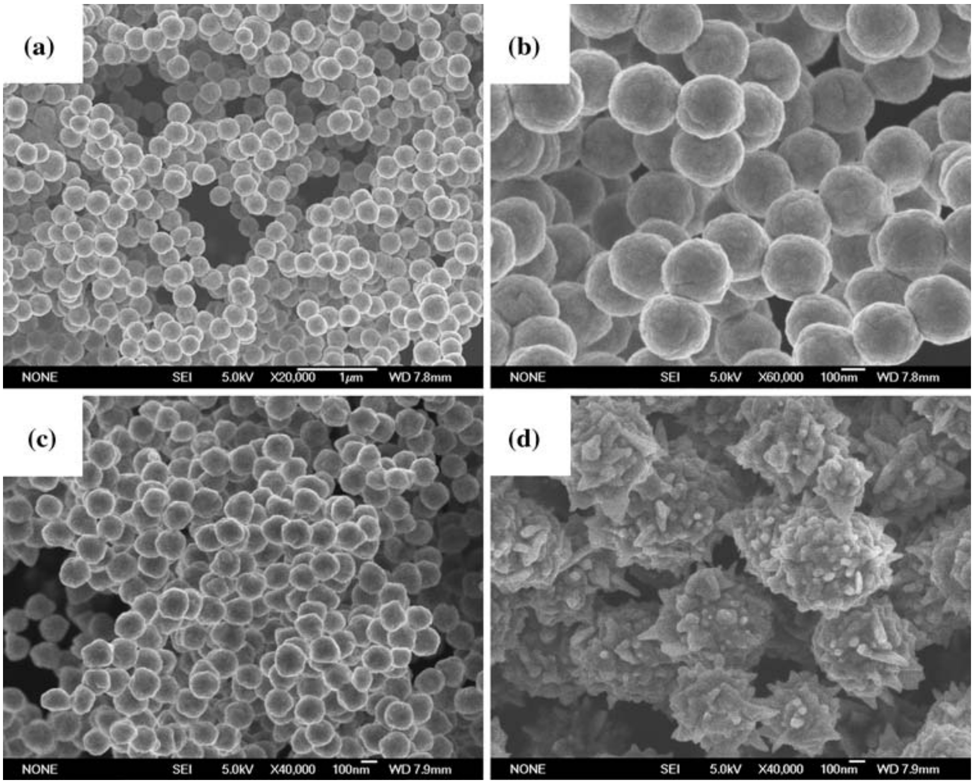

Fig. 3 FESEM images of the products obtained using water (**a**, **b**), ethylene glycol (**c**), and glycerin (**d**) as reaction media

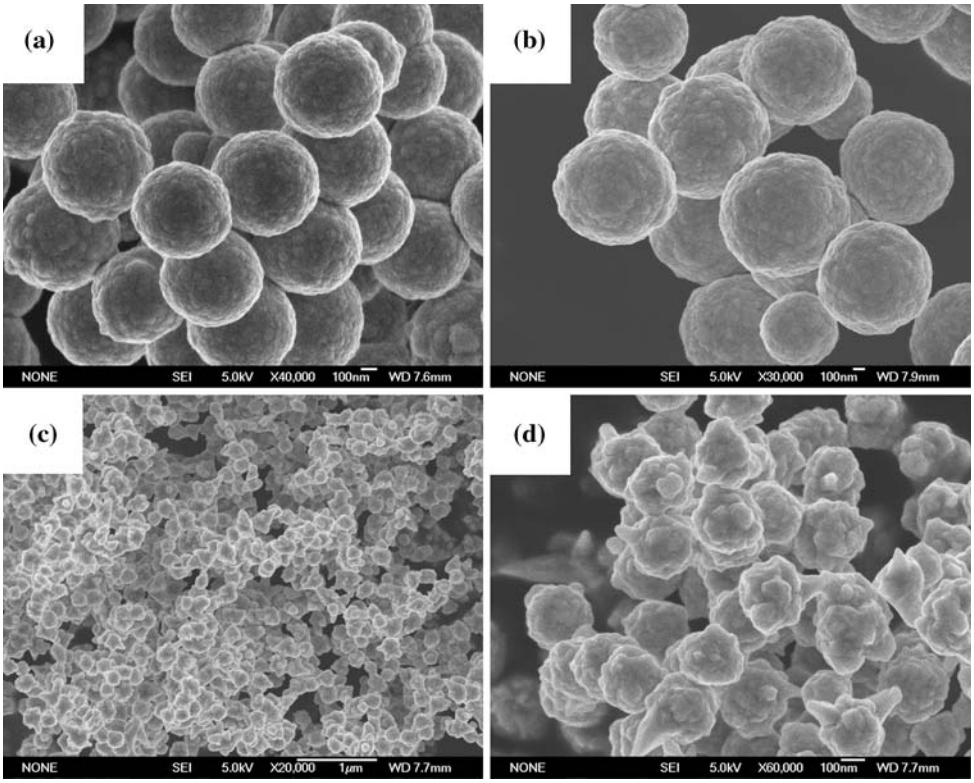

Fig. 4 (**a**, **b**) FESEM images of the products obtained with the concentrations of nickel at 0.075 and 0.05 M; (**c**, **d**) FESEM images of the products obtained with hydrazine concentration at 0.9 M

Along with the result (300 nm) at 0.1 M, it can be seen that the size of the nickel powders increases with decreasing of the initial nickel concentration. This result can be explained as follows: When the concentration of nickel was high, more nuclei were formed at the nucleation stage, which suppressed the growth of particles and led to the decrease of the average size of the products [20].

The effect of hydrazine concentration was also examined with the nickel concentration fixed at 0.1 M. It was found that a minimum hydrazine concentration was necessary to precipitate nickel from the solution. When hydrazine concentration was below 0.3 M, no nickel powders were formed using similar procedure. However, excessive hydrazine would deteriorate the morphology of the products. In addition, more water was brought into the system along with aqueous hydrazine, which might also cause the deterioration as mentioned above. Figure 4c and d shows the FESEM images of the products obtained with the concentration of hydrazine at 0.9 M. It can be seen that the particles are neither spherical in shape nor well dispersed. Therefore, a proper amount of hydrazine was necessary to get well-dispersed spherical nickel powders.

Effect of reaction time

It was found that nickel was recovered gradually from the solution. In order to obtain pure nickel and achieve a high yield ratio, sufficient reaction time is necessary. The yield ratio of nickel powders increases with the reaction time prolonged till 6 h. So 6 h is suitable for the preparation of pure nickel powders and the calculated yield ratio is almost 100%. Otherwise, the colorless post-reaction solution would provide another evidence for the high yield ratio. Figure 5 shows the FESEM images of nickel powders obtained for different reaction time. The morphologies are all spherical while the size increases from 200 to 300 nm as the reaction time prolonged from 4 to 6 h and keeps almost constant from 6 to 8 h. This result is consistent with that of the yield ratio.

Effect of reaction temperature

The chemical reduction was also performed at different temperature while keeping other conditions constant. Figure 6a and b shows the FESEM images of nickel powders obtained at 140 and 160 °C, respectively. The powders are both spherical in shape and well dispersed. The size is about 150 nm at 140 °C and about 250 nm at 160 °C. Along with the result (300 nm) at 120 °C, it can be seen that with the temperature raised, the size of the products increased first and then decreased.

The formation of nickel powders consists of three steps: formation of the primary particles, coalescence of them, and growth of the aggregates [21]. The size of the ultimate

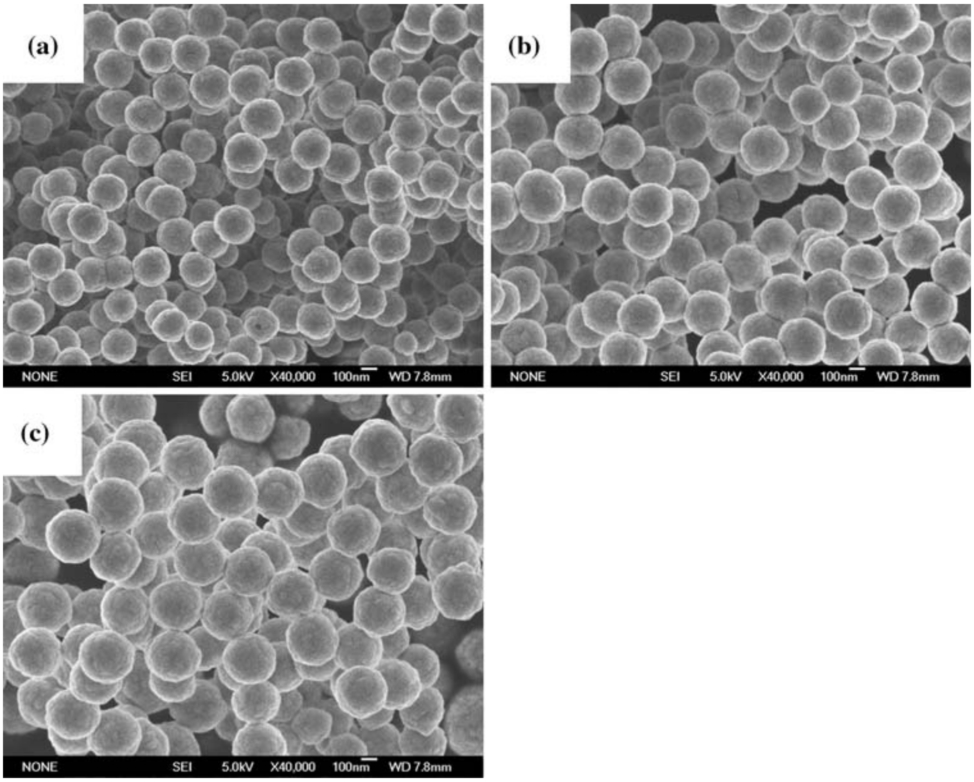

Fig. 5 FESEM images of the products obtained for different reaction time: **a** (4 h), **b** (6 h), and **c** (8 h)

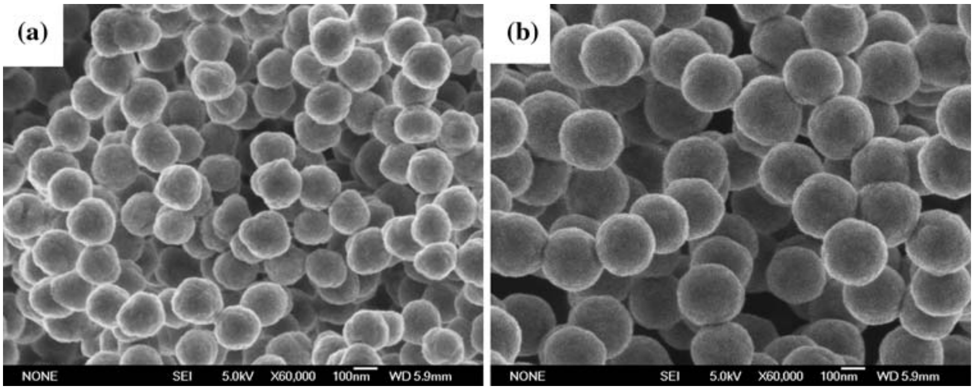

Fig. 6 FESEM images of the products obtained at 140 °C (**a**) and 160 °C (**b**)

powders is related to the number of the formed aggregates under a given condition. More aggregates lead to smaller size, which is also attributed to the suppression mechanism mentioned in section “Effect of concentration”. At a high temperature, the formation of the primary particles is fast at the initial stage of the reaction, which is helpful to form more aggregates. On the other hand, high temperature accelerates the diffusion and collision rate, which would help the coalescence and lead to the decrease of the number of the aggregates. So the size variation of the products was a result of the coordination of the two effects. As the temperature was raised from 120 to 140 °C, the acceleration of formation of the primary particles might be dominant. While the temperature was raised from 140 to 160 °C, the increase of coalescence rate might play the key role. Otherwise, glycerin might be involved in the reduction process at higher temperature, which would also influence the particle size of the nickel powders [22].

Powder characteristics

Figure 7 shows the XPS spectrum of the surface of the nickel powder obtained in glycerin at 120 °C for 6 h with the concentration of nickel and hydrazine at 0.1 and 0.6 M, respectively. Except for that of Ni confirmed by XRD patterns, photoelectron peaks associated to C and O peaks are present. Since no surfactant was introduced into the

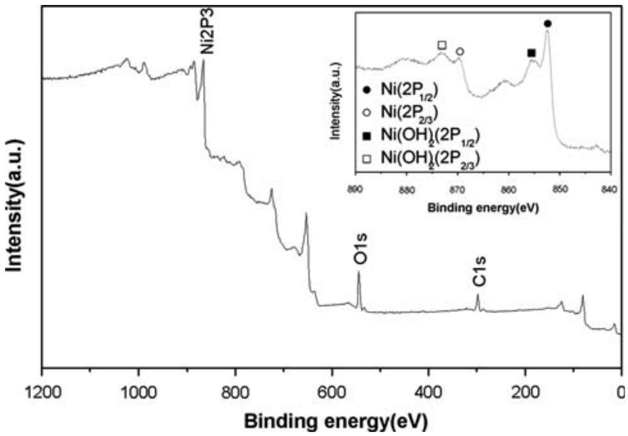

Fig. 7 XPS spectrum of the surface of the nickel powders (inset: narrow XPS scan of Ni2p)

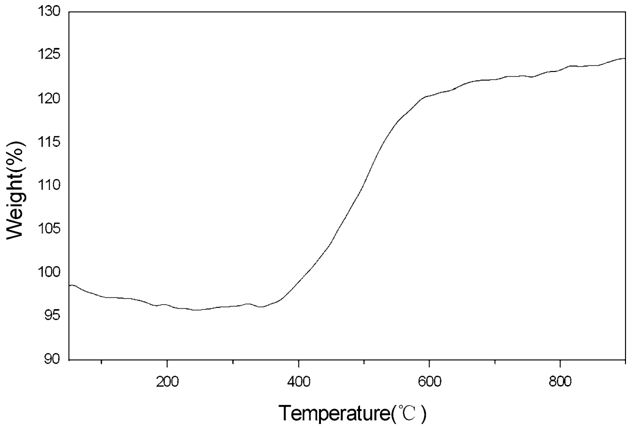

Fig. 9 TG curve of the nickel powders obtained in glycerin at 120 °C for 6 h

reaction system, the C and O peaks must originate from the organic solvent molecules adsorbed on the nickel powders, which could help form well-dispersed spherical nickel powders and prevent the formed nickel powders from oxidation. The inset spectrum shows the narrow XPS scan of Ni2p within the binding energy (BE) interval of 840–890 eV. A weak peak at about 856 eV exists along with the strong nickel peak at 852.6 eV. According to the literature [1], the weak peak could be attributed to the existence of $Ni(OH)_2$ on the surface of the nickel powders. But compared to that reported, the quantity of $Ni(OH)_2$ was much reduced due to the smaller peak area (PA). No NaOH was introduced into the reaction system and metallic nickel was recovered without existence of $Ni(OH)_2$, as shown in Eqs. 3 and 4. So $Ni(OH)_2$ on the surface of the nickel powders might be caused by the small quantity of water that was brought along with aqueous hydrazine and $NiCl_2 \cdot 6H_2O$. Figure 8b is the Narrow XPS scan of Ni2p of the nickel powders obtained from aqueous solution. Compared with that obtained in glycerin (Fig. 8a), the peaks of $Ni(OH)_2$ are much intensified and the peaks of Ni are weakened, indicating the increase of $Ni(OH)_2$ on the surface of the nickel powders. The use of glycerin instead of water as reaction media helped reduce the quantity of $Ni(OH)_2$.

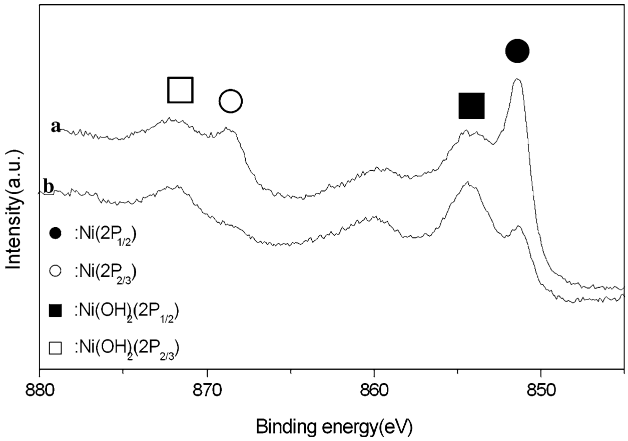

Fig. 8 Narrow XPS scan of Ni2p of the nickel powders obtained in glycerin (a) and in water (b)

Figure 9 shows TG curve of the nickel powders obtained in glycerin at 120 °C for 6 h. The weight loss occurs first with the temperature raised, which can be attributed to the loss of the organic compound and the decomposition of $Ni(OH)_2$ on the surface of the nickel powders. Then the weight gain starts at about 340 °C, indicating thermal oxidation of nickel powders begins at about 340 °C. The excellent oxidation resistance is also related to the high crystallinity of the obtained nickel powders as shown in Fig. 1.

Conclusion

In summary, we have successfully synthesized well-dispersed spherical nickel powders with uniform size, using aqueous hydrazine as reducing agent without any alkaline reagent or surfactant introduced. Solvent had great effect on the morphology of the products and glycerin could help the formation of well-dispersed nickel spheres. The reduction process was discussed on the basis of the experimental results. It was demonstrated that glycerin was not involved in the reduction reaction so it could be recycled as reaction media. The size of the spherical nickel powders ranges from 150 to 800 nm. The obtained nickel powders have little $Ni(OH)_2$ on the surface and exhibit excellent oxidation resistance.

Acknowledgements This work was supported financially by the National Natural Science Foundation of China (No. 50574083). One of the authors Liuyang Bai would thank Ms. Zhou for her assistance with FT-IR characterization.

References

1. Kim KH, Park HC, Lee SD, Hwa WJ, Hong SS, Lee GD, Park SS (2005) Mater Chem Phys 92:234
2. Park SH, Kim CH, Kang YC (2003) J Mater Sci Lett 22:1537
3. Kishi H, Mizuno Y, Chazono H (2005) AAPPS Bull 14:1
4. Shanmugavelayutham G, Selvarajan V (2004) Bull Mater Sci 27:453
5. Xia B, Lenggoro IW, Okuyama K (2001) J Mater Sci 36:1701
6. Ito T, Takatori H, U.S. Patent 6, 454, 830 B1
7. Park BK, Jeong S, Kim D, Moon J, Lim S, Kim JS (2007) J Colloid Interface Sci 311:417
8. Couto GG, Klein JJ, Schreiner WH, Mosca DH, de Oliveira AJA, Zarbin AJG (2007) J Colloid Interface Sci 311:461
9. Ghosh S, Ghosh M, Rao CNR (2007) J Cluster Sci 18:97
10. Ducamp-Sanguesa C, Herrera-Urbina R, Figlarz M (1993) Solid State Ionics 63–65:25
11. Fievet F, Lagier JP, Blin B, Beaudoin B, Figlarz M (1989) Solid State Ionics 32/33:198
12. Yu K, Kim DJ, Chung HS, Liang H (2003) Mater Lett 57:3992
13. Abdel-Aal EA, Malekzadeh SM, Rashad MM, El-Midany AA, El-Shall H (2007) Powder Technol 171:63
14. Gui Z, Fan R, Mo W, Chen X, Yang L, Hu Y (2003) Mater Res Bull 38:169
15. Jiang CL, Zou GF, Zhang WQ, Yu WC, Qian YT (2006) Mater Lett 60:2319
16. Li YD, Li CW, Wang HR, Li LQ, Qian YT (1999) Mater Chem Phys 59:88
17. Gao JZ, Guan F, Zhao YC, Yang W, Ma YJ, Lu XQ, Hou JG, Kang JW (2001) Mater Chem Phys 71:215
18. Guo L, Liang F, Wen X, Yang S, He L, Zheng W, Chen C, Zhong Q (2007) Adv Funct Mater 17:425
19. Kim KH, Lee YB, Choi EY, Park HC, Park SS (2004) Mater Chem Phys 86:420
20. Park JW, Chae EH, Kim SH, Lee JH, Kim JW, Yoon SM, Choi JY (2006) Mater Chem Phys 97:371
21. Shi WE, Chen ZZ, Yuan RL, Zheng YQ (2004) Hydrothermal crystallography. Science Press, Beijing
22. Bae D, Kim W, Kim S, Han K, Adair J (2001) J Mater Sci Lett 20:1969